

DESIGN AND MODELLING OF A $1 \times N$ ALL-OPTICAL NONLINEAR MACH-ZEHNDER SWITCH CONTROLLED BY WAVELENGTH AND INPUT POWER

Saeed Karimi, Majid Ebnali-Heidari*, and Farnaz Forootan

Faculty of Engineering, Shahrekord University, Shahrekord 8818634141, Iran

Abstract—The authors propose two $1 \times N$ all optical switches by taking the advantage of the accelerating behaviour of a spatial soliton in a Mach-Zehnder waveguide and the soliton's oscillating behaviour while propagating inside the nonlinear waveguide. The proposed switches consist of asymmetric and symmetric Mach-Zehnder waveguides followed by a homogenous Kerr medium, which is terminated by N parallel trapezoidal waveguides. In these switches, the signal is dropped from one of the desired output channels by changing the input pulse of wavelength or power. The numerical results confirm the switching application and show that the proposed $1 \times N$ switches can be used for wide ranges of wavelength and power, which are suitable for optical communication networks and optical data processing systems.

1. INTRODUCTION

Researchers are encouraged to design all optical devices in telecommunication industries due to their advantages such as ultra-high spectral bandwidth, great flexibility, and low attenuation. The development of all optical devices is too fast, as a result, variety of all optical devices such as switches [1–4], wavelength converters [5, 6], routers [7], modulator [8], gates [9], demultiplexers [10], and filters [11, 12] have been designed and produced recently. All-optical ultrafast photonic switches based on the nonlinear Kerr effect in an optical waveguide draw particular attention toward high-bit-rate optical communication systems and ultrafast information processing [13]. Optical switches

Received 5 October 2012, Accepted 26 December 2012, Scheduled 7 January 2013

* Corresponding author: Majid Ebnali-Heidari (ma.ebnali@gmail.com).

can change the signal path toward our desired output. In some waveguide based switches, by linear or nonlinear changing of the refractive indices in a homogenous Kerr medium of the waveguide and choosing a suitable wavelength and power of the input signal, the desired switch output channel is simply selected [14, 15]. Recently, soliton's oscillating behavior in nonlinear waveguides with different transverse index profiles has been studied [16–19]. In this paper, we propose a $1 \times N$ (input \times output) optical which includes three segments that in the first one both symmetric and asymmetric Mach-Zehnder waveguides are used. Mach-Zehnder is one of the most available optical interferometers, which we use on the first segment of proposed switches to make the phases difference at the output. And it also takes the advantage of the soliton's oscillating behavior while propagating inside the nonlinear waveguide in the second section and finally the last segment uses some output channels. This simple structure has many applications for signal switching to the desired output channel according to their wavelength and power. It also helps engineers to design all-optical broadband systems based on code division multiple access (CDMA) with many applications on third generation of cellular telecommunication network.

This paper is organized as follows: In Section 2, the physical models for two types of 1×5 Mach-Zehnder switches are proposed. Mathematical analysis is briefly presented in Section 3. Section 4 shows the simulation results using difference beam propagation method (FD-BPM) and finally Section 5 concludes the paper.

2. PHYSICAL MODEL

The schematic of our design, both asymmetric and symmetric Mach-Zehnder interferometer arms switch are displayed in Figures 1(a) and 1(b), respectively. In this figure the red and yellow marked are belong to nonlinear, and linear switch section, respectively. These structures comprise of three segments with various transverse refractive index profiles. The compound structures are followed by a homogeneous Kerr medium, which in turn is terminated by a trapezoidal waveguides. Each segment depending on its power and wavelength has a specified duty to control and guide its input signal toward next segment. Increasing the nonlinear refractive index in each segment caused by Kerr effect will increase the light intensities and leads to appear some nonlinear phenomena such as self-phase modulation (SPM). SPM leads to spectral broadening of the input pulse and simultaneously an important linear effect, which is called group velocity dispersion (GVD), results in temporal broadening. To

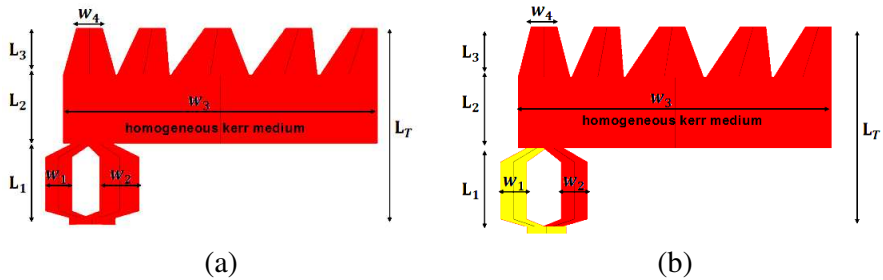


Figure 1. (a) 1×5 all-optical asymmetric Mach-Zehnder switch with nonlinear arms. (b) 1×5 all-optical symmetric Mach-Zehnder switch with linear-nonlinear arms.

prevent both SPM and GVD effects, soliton wave as the input signal is used. These waves propagate within a nonlinear medium without spectral and temporal broadening. This remarkable feature is due to the balancing of the wave's natural tendency to disperse with the opposing nonlinearity of the system. Solitons are special solutions of the nonlinear Schrödinger (NLS) equation that describe the paraxial propagation of an optical field in a Kerr medium [19–21]. All the segments have solitonic behaviors that cause the output signal to be unchanged.

The main reason for using nonlinear-nonlinear asymmetric and linear-nonlinear symmetric Mach-Zehnder arms as the input segment, is to create a phase difference between the received signals of the right and left arms and finally creating either constructive or destructive resultant signal at the next segment. The arms difference in both asymmetric and symmetric Mach-Zehnder is the source of the phase delay. The scheme employs angular deflection of spatial solitons controlled by phase modulation created in the Mach-Zehnder, which acts as a phase shifter. However, practical implementation of the structure shown in Figure 1(b) is simpler because of symmetric arms. The aim of using nonlinear Kerr medium as the second segment of the switch is to reduce the speed of propagating signal (speed of light), enhance the nonlinear effects, and create the signal swing mode which is completely discussed in [22]. All these approaches help signal guide toward one of the desired output channels in the last segment based on its power and wavelength. In both Figures 1(a) and 1(b) the output channels consist of five trapezoidal waveguides which are also extendable to N waveguides that is discussed in the following. However there are some other forms of waveguide, but trapezoidal one has advantage to prevent the disordered changing of the output

channel [23]. Moreover, these proposed switches have been designed according to international telecommunication union (ITU) standard. It means that the wavelength range of the first output channel is designed for C and L bands while the second output channel is designed for U-band.

3. FUNCTIONAL ANALYSIS

According to Section 2, the input pulse has the soliton shape as follows:

$$x(t) = P_0 \sec\left(\frac{T}{T_0}\right), \quad (1)$$

where P_0 , T_0 and T are the peak power, duration of the input pulse, and time parameter, respectively. Input pulse is launched into the first segment of switch. For simplicity and due to the non-periodic structure of the proposed $1 \times N$ switch, the TM and TE mode analyses are the same. So we consider the case of TE waves propagating along the structure as:

$$\varepsilon(x, z, t) = E(x, z) \exp[j(\omega t - \beta k_0 z)], \quad (2)$$

where k_0 is the wave number in free space, β the effective refractive index, ω the angular frequency, and E the electrical field of propagation signal. Also, the field has been assumed to be homogeneous in the y direction. Taking into account the slowly varying envelope approximation, $E(x, z)$ is obtained as follows [22, 23]:

$$2j\beta k_0 \frac{\partial E}{\partial z} + \frac{\partial^2 E}{\partial x^2} + k_0^2 \left[n_i^2(x, z, |E|^2) - \beta^2 \right] = 0. \quad (3)$$

For Kerr-type nonlinear medium, the total refractive index n_i can be written as [24]:

$$n_i = n_{i0} + n_{i1}I \quad (4)$$

In which n_{i0} and n_{i1} are the linear and nonlinear refractive indices of the nonlinear medium, and I is the signal intensity.

The phase difference between two Mach-Zehnder arms is given by [25]:

$$\Delta\phi = n_{i1}k_0L_1\Delta I \quad (5)$$

where L_1 is the length of Mach-Zehnder optical path (according to Figure 1) and ΔI the intensity difference between two received signals of both arms. $\Delta\phi$ is an important parameter to define the output intensity in each position at the output of the first segment. For example $\Delta\phi$ equals to 0 and 180° , results in constructive and destructive fields, respectively. The constructive field effect just happens in a special position which determines the signal path at the next segment.

4. NUMERICAL RESULTS AND DISCUSSIONS

In this section, the switches performance and applications are numerically investigated. For simulation of the signal propagation along proposed switches finite difference beam propagation method (FD-BPM) [26, 27] is used. There are several reasons for selecting the FD-BPM; one of the most significant reasons includes that it is conceptually straightforward, which allows rapid implementation of the basic technique. This conceptual simplicity also benefits the user of the FD-BPM based modeling tool as well as the implementer, since an understanding of the results and proper usage of the tool can be readily grasped by a non-expert in numerical methods. In spite of the relative

Table 1. The device parameters for both structures shown in Figure 1.

Description	L_1 (μm)	L_2 (μm)	L_3 (μm)	L_T (μm)
Figure 1(a)	2400	2000	1400	5800
Figure 1(b)	2400	2000	1400	5800
Description	W_1 (μm)	W_2 (μm)	W_3 (μm)	W_4 (μm)
Figure 1(a)	2 Nonlinear arm	3 Nonlinear arm	24	2
Figure 1(b)	2 Linear arm	2 Nonlinear arm	24	2

Table 2. The output channel number versus the wavelength range of the input signal for P_0 equals to 18 W for both proposed switches as illustrated in Figure 1.

Output	Channel #1	Channel #2	Channel #3
Figure 1(a) wavelength (μm)	1.5–1.645	1.645–1.730	1.731–1.90
Figure 1(b) wavelength (μm)	1.5–1.660	1.661–1.825	1.826–1.833
Output	Channel #4	Channel #5	-
Figure 1(a) wavelength (μm)	1.901–2	2.001–2.05	-
Figure 1(b) wavelength (μm)	1.834–2.031	2.032–2.05	-

simplicity, FD-BPM is generally an efficient method, which makes the characteristic of computational complexity optimal in most cases, i.e., the computational effort is directly proportional to the number of grid points used in the numerical simulation. Another characteristic of FD-BPM method is that the approach is readily applied to complex geometries without any necessity to develop specialized versions of it. Furthermore, the approach automatically includes the effects of both guided and radiating fields as well as mode coupling and conversion. Finally, the -FBPM technique is very flexible and extensible, allowing inclusion of most effects of interest (e.g., polarization, nonlinearities) by extensions of the basic method that fit within the same overall framework. The device parameters and values related to both proposed switches are given in Table 1 in which L_1 , L_2 and L_3 are the lengths of the first, second and third segments of the switch, respectively. W_1 and W_2 are the left and right arm widths of the Mach-Zehnder waveguide. W_3 is the width of the second segment (homogenous Kerr medium) and W_4 the width of each channel of the output segment. In the first simulation related to structure shown in Figure 1(a), the peak power of the input pulse was kept as a constant value of 18 W, and only its wavelength is changed from $1.5 \mu\text{m}$ to $2.05 \mu\text{m}$. Here the proposed switches rely on the wavelength variations, which causes phases difference in the first output segment of the switches and the signal to appear in different spatial locations of Mach-Zehnder output. This difference along with second segment swing properties causes the signal to extract in different channels due to input power and wavelength. The evolutions of such a input pulse with constant power propagating along 1×5 all-optical switch are demonstrated in Figure 2. Figure 2 and Table 2 reveal that when input signal wavelength is between $1.5 \mu\text{m}$ to $1.645 \mu\text{m}$, the coupled signal passes from channel #1. For another case with wavelength between $1.645 \mu\text{m}$ to $1.73 \mu\text{m}$, it passes from channel #2. The other results of the switch function related to wavelength ranges according to Table 2 present in Figures 2(c), 2(d), and 2(e). One of the most important characteristic of the designed switch is that by increasing the wavelength of the input signal, it sequentially switches to the output channel as desired which is demonstrated in Figure 2 and Table 2. Moreover, the simulations were repeated for the second structure shown in Figure 1(b) with the same peak power as mentioned above, and the results are given in Table 2 in which they also confirm that increasing the input signal wavelength shifts it toward the output channel sequentially, which means that by using symmetric Mach-Zhender, beside easier and cheaper fabrication process, similar results to the asymmetric one are obtained.

Our simulations are followed for the case where the input signal

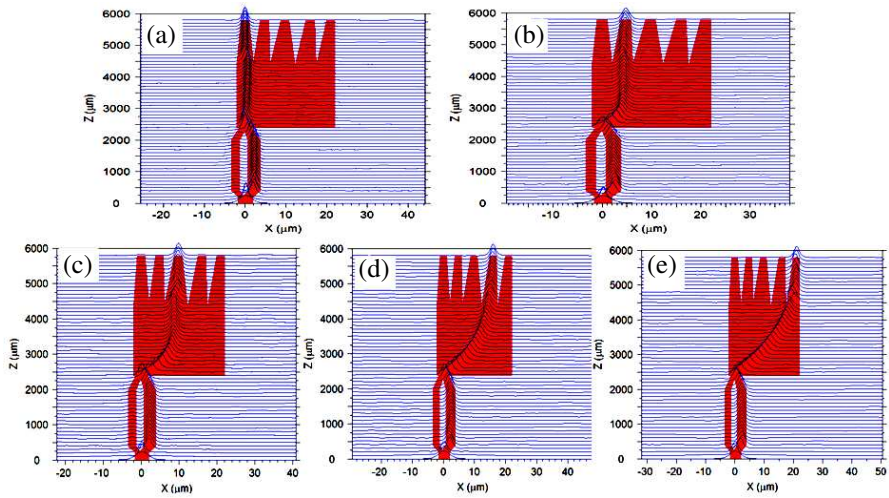


Figure 2. The evolutions of the input pulse propagating along 1×5 all-optical switch based on Figure 1(a) for constant power of 18 W and wavelength range of the input signal from (a) $1.5 \mu\text{m}$ to $1.645 \mu\text{m}$, (b) $1.645 \mu\text{m}$ to $1.73 \mu\text{m}$, (c) $1.731 \mu\text{m}$ to $1.9 \mu\text{m}$, (d) $1.901 \mu\text{m}$ to $2 \mu\text{m}$ and (e) $2.001 \mu\text{m}$ to $2.05 \mu\text{m}$.

Table 3. The output channel number versus the peak power of the input signal for a constant wavelength of $1.55 \mu\text{m}$.

Output	Channel #5	Channel #4	Channel #3
Figure 1(b) Input peak power (W)	10–10.62	10.63–11.53	11.54–13.18
Figure 1(a) input peak power (W)	10–12.99	13–13.48	13.49–14.67
Output	Channel #2	Channel #1	-
Figure 1(b) Input peak power (W)	13.19–15.31	15.32–40	-
Figure 1(a) input peak power (W)	14.68–15.77	15.78–40	-

wavelength is assumed to be constant with $1.55\ \mu\text{m}$, and its only peak power changes from 10 to 40 W. Here as before, the simulations are repeated for both structures of Figure 1, and the results of simulation for both Figures 1(a) and 1(b) are given in Table 3. Moreover, the input pulse propagation along switch shown in Figure 1(b) is depicted in Figure 3 for different values of its peak power as Table 3.

Figure 3 also shows and confirms that just by changing the input signal peak power, the desired output channel will be obtained. According to the results of Table 3, for fixed wavelength of the input signal, both switches have the same behaviour. So we prefer to use the second one because of the easier and cheaper fabrication process.

The signal position shifts versus the wavelength for different values of the input peak power are calculated, and finally the related curves for both structures are depicted in Figure 4.

According to Figure 4(a), related to the first structure, the most position shift occurs at $p = 17.9\ \text{W}$; however there is not any positions shift in Figure 4(b), related to the second one, in that power and range

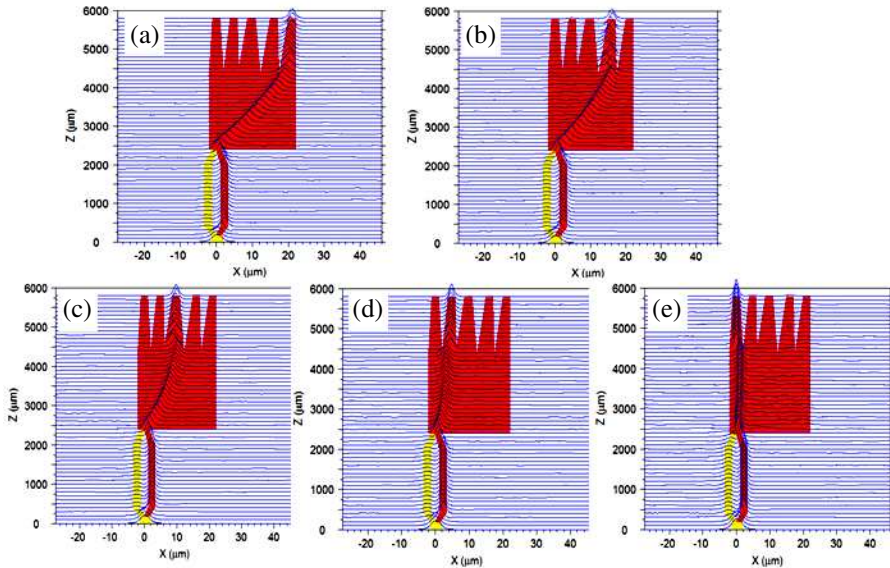


Figure 3. The evolutions of the input pulse propagating along 1×5 all-optical switch based on Figure 1(b) for constant wavelength equals to $1.55\ \mu\text{m}$ and power range of the input signal from (a) 10 W to 1.62 W, (b) 10.63 W to 11.53 W, (c) 11.54 W to 13.18 W, (d) 13.19 W to 15.31 W and (e) 15.32 W to 40 W.

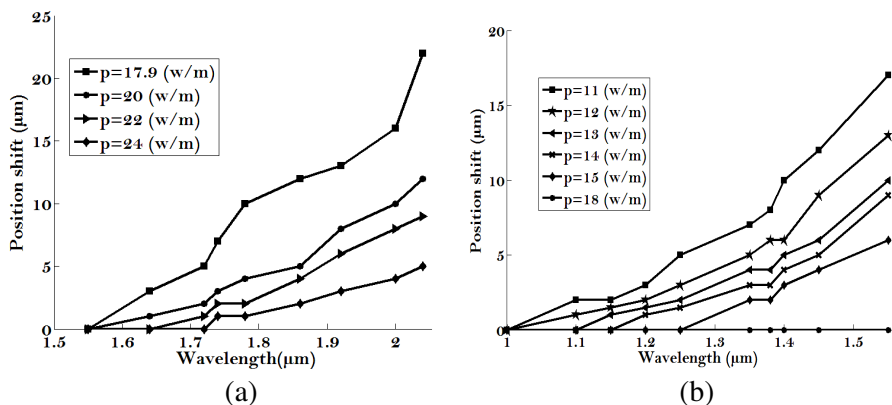


Figure 4. (a) Position shift versus wavelength in different values of the input power for structure as Figure 1(a). (b) Position shift versus wavelength for different values of input power for structure as Figure 1(b).

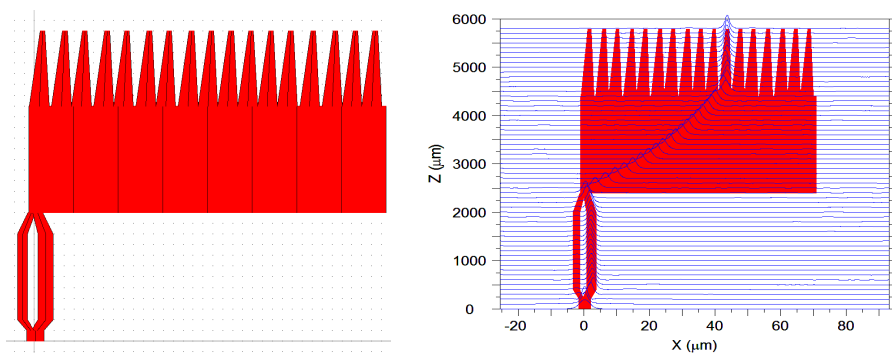


Figure 5. A $1 \times N$ all-optical nonlinear Mach-Zehnder switch.

of the wavelength. The simulation results curves also show that the switch in the condition of Fig. 4(b) can work in lower powers than that in the situation of Fig. 4(a) for the same position shift which is another reason for choosing the second switch as desired. Figures 4(a) and 4(b) show that by increasing the input peak power, the position shift is reduced; however the curves are almost linear. Linear curves help us extend our method to design a $1 \times N$ switch as illustrated in Figure 5 by N trapezoidal waveguides.

Now, for an optimal design of switch, the length of homogeneous Kerr medium for both symmetric and asymmetry $1 \times N$ all optical

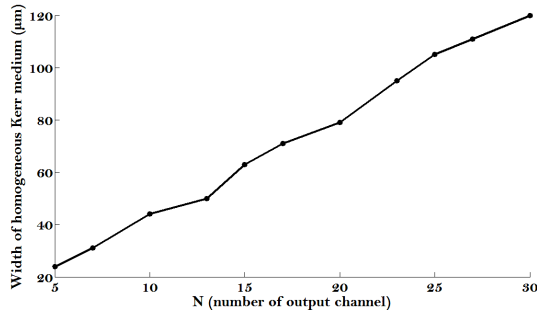


Figure 6. Width of homogeneous Kerr medium versus number of output channel (from $N = 5$ to $N = 30$).

switches should be computed. In the proposed switches, X_T is a place in homogeneous Kerr medium that the signal propagates directly from the first segment toward the last output channel without any variations. The design rule for $1 \times N$ channel switch is based on generalizing switch 1×5 and repetition of second segment and output channels until it reaches $1 \times N$ switch channel. According to our simulations for mentioned switches consisting of five-channel output, X_T is $24 \mu\text{m}$, and for another switch with ten-channel output, it is around $46 \mu\text{m}$, which means that by increasing the number of output channels by a factor of two, the width of homogeneous Kerr medium is approximately doubled. By repeating our simulations for many switches with different numbers of output channels, we can generalize the principle for N -channel output switch as follows:

$$x_T (\mu\text{m}) \approx 4N \quad (6)$$

where N is the number of output channel.

5. CONCLUSION

We propose two all optical switches controlled by both input peak power and wavelength. Each one includes a Mach-Zehnder waveguide followed by a homogenous Kerr medium, which in turn was terminated by N parallel trapezoidal waveguides. The Mach-Zehnder waveguide was symmetric for one of them and asymmetric for the other one. The numerical results showed that the signal was dropped from one of the desired output channels by changing either the wavelength of input pulse or power. They also confirmed that the proposed switches can be used for wide range of wavelength and power, which makes the device suitable for optical communication networks and optical data

processing systems. We also showed that the switch can be utilized to be a $1 \times N$, by either reducing the widths of output channels or increasing the length of the Kerr medium as the proposed equation which is obtained by the simulation results.

REFERENCES

1. Nakamura, H., Y. Sugimoto, and K. Asakawa, "Ultra-fast photonic crystal/quantum dot all-optical switch for future photonic networks," *Optics Express*, Vol. 12, No. 26, 6606–6614, 2004.
2. Beggs, D. M., et al., "Ultra compact and low-power optical switch based on silicon photonic crystals," *Optics Letters*, Vol. 33, No. 2, 147–149, 2008.
3. Cho, S. Y. and R. Soref, "Interferometer microring-resonant 2×2 optical switches," *Optics Express*, Vol. 16, No. 17, 13304–13314, 2008.
4. Ridolfo, A., et al., "All optical switch of vacuum Rabi oscillations: The ultrafast quantum eraser," *Phys. Rev. Lett.*, Vol. 106, No. 1, 013601, 2011.
5. Lal, V., et al., "Monolithic wavelength converters for high-speed packet-switched optical networks," *IEEE Journal of Selected Topics in Quantum Electronics*, Vol. 13, No. 1, 49–57, 2007.
6. Ebnali-Heidari, M., M. K. Moravvej-Farshi, and A. Zarifkar, "Multi channel wavelength conversion using fourth-order soliton decay," *Journal of Lightwave Technology*, Vol. 25, No. 9, 2571–2578, 2007.
7. Sherwood-Droz, N., et al., "Optical 4×4 hitless silicon router for optical networks-on-chip (NoC)," *Optics Express*, Vol. 16, No. 20, 15915–15922, 2008.
8. Bakhshi, S., M. K. Moravvej-Farshi, and M. Ebnali-Heidari, "Design of an ultracompact low-power all-optical modulator by means of dispersion engineered slow light regime in a photonic crystal Mach-Zehnder interferometer," *Applied Optics*, Vol. 51, No. 14, 2687–2692, 2012.
9. Lai, D. M., C. Kwok, and K. K. Wong, "All-optical picoseconds logic gates based on a fiber optical parametric amplifier," *Optics Express*, Vol. 16, No. 22, 18362–18370, 2008.
10. Gayen, D. K. and J. N. Roy, "All-optical arithmetic unit with the help of terahertz-optical-asymmetric-demultiplexer-based tree architecture," *Applied Optics*, Vol. 47, No. 7, 933–943, 2008.

11. Tu, X., F. Liu, and N. Xu, "Design of high channel-count optical fiber filters based on sampled Bragg grating with discrete linear chirp structure," *Optics and Precision Engineering*, 2010.
12. Bitarafan, M., M. Moravvej-Farshi, and M. Ebnali-Heidari, "Proposal for postfabrication fine-tuning of three-port photonic crystal channel drop filters by means of optofluidic infiltration," *Applied Optics*, Vol. 50, No. 17, 2622–2627, 2011.
13. Lu, H., et al., "Ultrafast all-optical switching in nanoplasmonic waveguide with Kerr nonlinear resonator," *Optics Express*, Vol. 19, No. 4, 2910–2915, 2011.
14. Wu, Y. D., et al., "All-optical switch based on the local nonlinear Mach-Zehnder interferometer," *Optics Express*, Vol. 15, No. 16, 9883–9892, 2007.
15. Camargo, E., H. Chong, and R. de la Rue, "2D photonic crystal thermo-optic switch based on AlGaAs/GaAs epitaxial structure," *Optics Express*, Vol. 12, No. 4, 588–592, 2004.
16. Garzia, F., C. Sibilia, and M. Bertolotti, "Swing effect of spatial soliton," *Optics Communications*, Vol. 139, No. 4–6, 193–198, 1997.
17. Suryanto, A. and E. van Groesen, "On the swing effect of spatial inhomogeneous NLS solitons," *Journal of Nonlinear Optical Physics and Materials*, Vol. 10, No. 2, 143–152, 2001.
18. Suryanto, A. and E. van Groesen, "Break up of bound- N -spatial-soliton in a ramp waveguide," *Optical and Quantum Electronics*, Vol. 34, No. 5, 597–606, 2002.
19. Moravvej-Farshi, M., M. E. Heidari, and A. Zarifkar, "Spatial solitons in compound ramp waveguides," *Proceedings of CAOL 2005 Second International Conference on Advanced Optoelectronics and Lasers*, Vol. 2, 160–163, 2005.
20. Agrawal, G. P., *Nonlinear Fiber Optics*, 2nd Edition, Academic Press, 2001.
21. Agrawal, G. P., *Fiber Optic Communication Systems*, Wiley-Interscience, 2002.
22. Ebnali-Heidari, M., M. K. Moravvej-Farshi, and A. Zarifkar, "Swing effect of spatial solitons propagating through Gaussian and triangular waveguides," *Applied Optics*, Vol. 48, No. 26, 5005–5014, 2009.
23. Aceves, A. B., J. V. Moloney, and A. C. Newell, "Theory of light-beam propagation at nonlinear interfaces. I. Equivalent-particle theory for a single interface," *Phys. Rev. A*, Vol. 39, 1809–1827, 1989.

24. Kuo, C. W., et al., "Analyzing multilayer optical waveguide with all nonlinear layers," *Optics Express*, Vol. 15, No. 5, 2499–2516, 2007.
25. Berrettini, G., et al., "Ultrafast integrable and reconfigurable XNOR, AND, NOR, and NOT photonic logic gate," *IEEE Photonics Technology Letters*, Vol. 18, No. 8, 917–919, 2006.
26. Niwa, S., et al., "Experimental demonstration of 1×4 InP/InGaAsP optical integrated multimode interference waveguide switch," *20th International Conference on Indium Phosphide and Related Materials, 2008, IPRM 2008*, 1–4, 2008.
27. Scarmozzino, R., et al., "Numerical techniques for modeling guided-wave photonic devices," *IEEE Journal of Selected Topics in Quantum Electronics*, Vol. 6, No. 1, 150–162, 2000.